Prototype-scale field investigation of regulated water-jet pile pressing in dense sand

G.N. Meshcheriakov
Engineering Center Transzvuk, Odesa, Ukraine, ectranszvuk@gmail.com

ABSTRACT: This paper presents the results of a prototype-scale field investigation of a pile-pressing method enhanced with regulated water jetting for precast reinforced concrete piles in dense sand. The study addresses key challenges in foundation construction for low- and medium-rise buildings and highlights its integration into construction automation. Field experiments performed with an automated pile-pressing machine and various jetting configurations showed that regulated jetting reduced pressing resistance by 55–70 % and enabled penetration up to 1.7 m under the same pressing force of 1834 kN. A mechanistic interpretation of the observed stick–slip effect is proposed as a piston-type hydraulic hypothesis derived from recorded pressing force oscillations during installation. Static load tests indicated that jetting did not compromise axial bearing capacity: settlements under a 700 kN load were 2.2 mm for the control pile and 3.5 mm for the jetted pile, and the allowable load of 466.6 kN satisfied the design safety factor of 1.2. Although the statistical basis of static testing is limited by regulatory requirements, no reduction in axial bearing capacity was observed under the investigated site conditions. Complementary 1-g tests qualitatively demonstrated that regulated jetting with controlled slurry removal mitigates stick–slip behavior. The results provide prototype-scale field evidence of a controllable hydraulic interaction mechanism under real construction constraints.

1 INTRODUCTION

Pile-pressing technology offers a rapid, reliable, and environmentally compatible foundation solution by minimizing disturbance to the surrounding ground and existing infrastructure. However, in dense sandy soils, the required reaction forces may exceed the capacity of the piling equipment, leading to premature refusal and the need for costly pre-boring.

Water-assisted installation techniques have been widely applied for steel sheet piles and tubular piles, but their use for precast reinforced concrete piles remains insufficiently validated. These piles differ fundamentally from metallic profiles in stiffness, geometry, and soil–pile interaction behavior, particularly due to the absence of interlock friction and plugging effects. Although high-pressure jetting has been used in offshore engineering, its adaptation for precast concrete piles in civil construction has not been systematically examined.

A particular challenge in the water-jet-enhanced pile-pressing method is the stick–slip phenomenon—a cyclic instability characterized by alternating phases of resistance build-up and sudden acceleration caused by pore-pressure increase and abrupt soil fluidization. This instability poses not only a geotechnical concern but also a critical operational hazard for automated pile-pressing machines, especially those equipped with side-clamp systems.

Such impulsive loads interfere with the control feedback of automated systems, undermining process stability and safety. While observed in laboratory and centrifuge studies, its mechanism and controllability for full-scale installations of precast reinforced concrete piles remain poorly understood.

This study, therefore, examines three hypotheses:

- Water jetting significantly reduces pressing resistance by decreasing side friction during precast pile installation in dense sand;
- Regulated jetting does not adversely affect the load-bearing capacity of piles relative to the conventional pressing method;
- The effectiveness of jetting depends not only on water pressure but also on flow regulation and effective slurry management.

To address these hypotheses, the study adopts a hybrid experimental framework combining field investigation under active construction conditions, mechanism-oriented 1-g testing, and analytical interpretation of pile–water–soil interaction. The program employed a regulated pile–piston regime using the SO-450 pile-pressing machine.

In contrast to classical stress-scaled centrifuge modelling, the objective is not strict similitude but documentation of hydraulic behaviour during pile installation at full engineering scale.

2 LITERATURE REVIEW

The concept of using water jetting to facilitate pile penetration dates back to the 1950s. Early full-scale tests by the U.S. Army Corps of Engineers (1962) demonstrated that jetting could reduce penetration time by up to 75 % when installing concrete piles in dense sands, but also caused 10–35 % losses in axial load-bearing capacity, mainly due to uncontrolled soil loosening. This unfavorable outcome shaped the long-standing skepticism toward this method.

Later research (Tsinker, 1988) demonstrated that water-induced soil fluidization reduces pile side friction by about 20–30 % and end-bearing resistance by 40–60 %. Uncontrolled fluidization was found to excessively weaken the bearing layer and ultimately reduce the pile's load-bearing capacity.

Full-scale research on water-jetted installation of precast concrete piles has remained limited. Field experiments (Gunaratne et al., 1999) reported that water-jetting reduced shaft resistance in PHC piles by about 30–35 %, but that capacity could be restored or exceeded through post-grouting. More recent field experiments showed that PHC screw piles (Ø 400 mm), installed into dense sand with 8–12 MPa jetting, achieved up to 45 % resistance reduction and 1.6 m deeper penetration, without capacity loss.

Research on steel sheet piles (Gillow et al., 2018) highlighted that penetration rate was governed mainly by jetting pressure (> 6 MPa) rather than by flow rate, enabling faster installation but requiring water consumption up to 1500 L per sheet pile. However, they also noted that for small-diameter jet nozzles (Ø < 2 mm), the flow rate becomes a significant controlling factor.

Summarizing early field observations, it was noted (Malhotra, 2004) that uncontrolled jetting can reduce pile capacity by 80–90 % when slurry is discharged externally along the shaft and by 20–25 % when it is discharged internally through the pile core, due to the loss of confinement in surrounding sand.

Small-scale model studies have provided detailed insight into soil fluidization mechanisms (Passini et al., 2015, 2018). Experiments on tubular piles (Ø 25–75 mm) in medium-dense saturated sand using vertical jets at 0.2–1.0 MPa showed that penetration ratios L/d > 50 can be achieved, compared with < 5 without jetting, and they derived a non-dimensional embedment law based on the Froude number. Consistent with these findings, it was experimentally confirmed that the radius of the fluidized zone remains approximately twice the pile diameter, independent of sand density (Mezzomo, 2009).

Centrifuge experiments (White and Bolton, 2004) identified alternating phases of shaft resistance buildup and loss, associated with transient pore-pressure generation. Subsequent studies (Shepley and Bolton, 2013) confirmed that these intermittent reductions in resistance correspond to pore-pressure oscillations of 0.2–0.4 MPa beneath the pile toe.

Laboratory tests in soft clays (Liu et al., 2020) documented similar behavior, characterized by sudden displacement jumps of 3–4 mm within 0.3 s, while jetting reduced the amplitude of these jumps by about 35–40 %. More recent centrifuge studies (Maiti and Shepley, 2025) extended these findings to submerged granular beds, showing that maintaining a confined, localized fluidized zone suppresses force oscillations, stabilizing penetration.

Geometric modification of the pile toe has been proposed as a means to restore or enhance capacity after jetting. Numerical and experimental results (Ruver and Bruschi, 2023) demonstrated that ribbed and under-reamed geometries can increase load-bearing capacity by 30–80 % depending on soil conditions. However, these geometric adjustments do not fully address the hydraulic instability arising from unregulated pore-pressure buildup.

Most previous studies have focused on tubular and sheet piles, where interlock friction and soil plugging dominate the response. While centrifuge and laboratory investigations have significantly advanced understanding of jet-induced fluidization, full-scale experimental evidence for precast concrete piles remains limited. In particular, the combined operation of regulated water jetting and automated pile-pressing equipment has not been systematically documented. The present study provides prototype-scale field data addressing this gap while acknowledging the methodological constraints inherent to in-situ experimentation.

3 RESEARCH METHODOLOGY

3.1 Site description

Full-scale experiments were conducted at the site of the Kuchurgan Branch of the Odessa Baby-Food Canning Plant in the Odesa Region between 23 May and 6 June 2024. The test area consisted of a leveled rectangular site (50 × 30 m) with a surface elevation of approximately +7.0 m, surrounded by existing industrial facilities. The construction contract at this site provided the opportunity to evaluate the regulated water-jetting technique under realistic industrial conditions in a dense sandy soil profile.

Groundwater was encountered at a depth of 3.0–3.5 m below ground level, and the seismicity of the site corresponds to MSK-64 intensity VIII.

3.1.1 Piling equipment

Pile pressing operations were performed using the SO-450 automated hydraulic piling machine, with a maximum pressing force of 2000 kN (200 tf). It was adapted for both pile installation and static load testing, ensuring continuous monitoring of pressing parameters throughout the experiments. A 25-ton crane was employed, as illustrated in Figure 1.

Figure 1. Crane-assisted placement of the piling machine

3.1.2 Soil profile and properties

The soil profile at the construction site comprises four engineering–geological elements (EGE), whose physical and mechanical properties are essential for analyzing pile behavior:

- EGE-1 (0–1.5 m) – technogenic black silty sand containing organics and petroleum residues: unit weight γ = 16.0 kN/m³, internal friction angle φ = 28°, permeability coefficient k = 5×10^{-5} m/s, deformation modulus E = 5 MPa; loose; layer was used for small-scale testing, where model tubular piles were installed.
- EGE-2 (1.5–4.0 m) – yellow-brown fine quartz sand of medium density, located below the groundwater level: γ = 17.6 kN/m³, φ = 34°, k = 1.3×10^{-4} m/s, E = 18 MPa; represents the first water-saturated horizon and initial pressing zone.
- EGE-3 (4.0–6.0 m) – grey fine sand with interbedded soft clayey-silt lenses, medium-dense: unit weight γ = 17.8 kN/m³, φ = 34°, k = 1.1×10^{-4} m/s, E = 20 MPa; this layer transmits side friction up to control pile refusal.
- EGE-4 (6.0–8.5 m) – brown-yellow medium quartz sand, dense and saturated: γ = 18.5 kN/m³, φ = 36°, k = 1.3×10^{-4} m/s, E = 26 MPa, relative density D_r = 75%; serves as the bearing layer where all project piles are embedded and where the water-jet effect is most pronounced.

3.2 Experimental phases and data acquisition

The research program was organized into four sequential phases (P) to evaluate the effects of pile pressing enhanced by regulated water jetting and to provide field-based experimental validation at both prototype and model scale:

- P1 – two control piles were installed without jetting to establish baseline soil resistance and determine the refusal point;
- P2 – sixteen project piles were installed with water jetting (modes a, b) to a target depth of 7.7 m, under the course of construction;
- P3 – four piles (two control and two jetted) were tested under static loading to verify axial load-bearing capacity;
- P4 – model tubular piles were manually installed and extracted using jetting to study stick–slip and soil fluidization mechanisms.

Within P2, two operational configurations were implemented: (a) continuous jetting mode — an open hydraulic circuit with a constant-rate water supply through the jet nozzle; (b) regulated pile–piston regime — after the pump relief activation, the pile was uplifted by machine to 0.3–0.4 m, creating a closed water-filled cavity beneath the pile tip.

The following parameters were recorded: pressing force (kN/tf), penetration depth (m), pressing speed (m/min), and total installation time (min). For jetted piles and models, water supply cycles were logged, marking the onset and termination of jetting. Jetting parameters included flow rate (L/min and L/pile), water pressure (bar/MPa), and nozzle diameter.

3.3 Static load tests

The reaction system consisted of the SO-450 pressing machine acting as a reaction frame and a stacked counterweight totaling 180 t (18 blocks of 10 t each). The static load was applied incrementally in 100 kN steps up to a maximum of 700 kN.

At each test cycle, the load (kN), settlement (mm), and elapsed time were recorded. Stabilization periods were maintained until the settlement rate dropped below 0.1 mm per 30 minutes, allowing evaluation of creep behavior. Unloading–reloading cycles were included to distinguish elastic and plastic deformation components. Settlements was measured by two 6ПАО deflectometers (resolution 0.01 mm) placed symmetrically 1.5 m from the pile axis, while the applied load was monitored with a hydraulic manometer (range 400 atm, resolution 5 atm). The ultimate bearing capacity was determined based on settlement-based failure criteria.

3.4 Pile geometry and jetting system

Prismatic concrete piles (C90.35-10) with a 350 × 350 mm cross-section and a length of 9 m were factory-cast from C25/30 concrete and reinforced with Ø18 mm A400C steel bars. To facilitate water-jetting, each pile was equipped with a centrally positioned steel pipe (DN15) running along its full length and ending in a multi-orifice nozzle (Ø2 mm) at the pile tip, as illustrated in Figure 2.

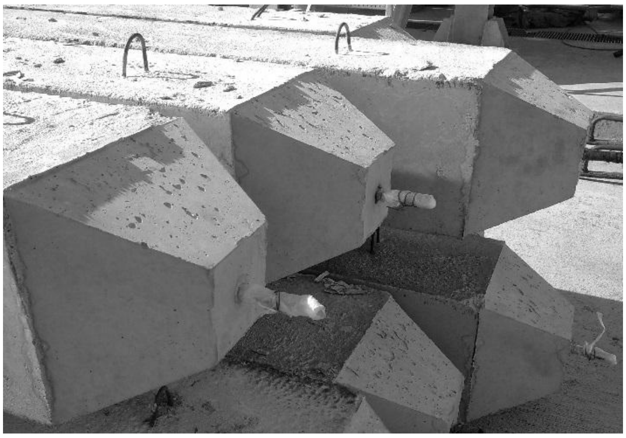

Figure 2. Concrete piles with integrated jet nozzles

A high-pressure hose connection for water supply was integrated at the pile head. A high-pressure pump (K HD 6/15 C) 3.1 kW, with a capacity of 9.3 L/min and a maximum pressure of 15 MPa (150 bar) with pump relief activation at approximately 16 MPa, was used throughout phases 2 and 4.

3.5 Tubular pile models

A series of 1-g model pile tests (P4) was conducted as a qualitative feasibility study to examine penetration under regulated water jetting, aiming to explore hydraulic instability mechanisms and evaluate operability of the anti-plugging geometry.

The tests were performed in the surface layer (EGE-1) available on site. Model piles consisted of Ø100 mm steel pipes (2 m long) with a closed toe and a centrally installed DN15 water-supply pipe. A crosspiece with a manual handle at the pile head enabled controlled installation and extraction. Two model piles (M) were tested, representing different flow-control principles.

- M1 – reproduced the continuous (constant-rate) water–jetting regime. The high-pressure hose was connected directly to the internal pipe at the pile head, supplying water to a Ø2 mm multi-orifice jet nozzle, identical to that used in the full-scale tests, fixed at the tip, as illustrated in Figure 3.
- M2 – the nozzle at the pile tip (M1) was cut off, creating a through cavity along the entire length of the tubular pile. A flexible hose with a multi-orifice Ø0.7 mm jet nozzle was inserted through this cavity to the pile tip, enabling regulated jetting and simultaneous slurry removal from the under-tip zone.

Figure 3. Model tubular pile (M1), where: 1 – steel pipe with closed lower end; 2 – jet nozzle; 3 – internal pipe.

Three penetration and extraction cycles in EGE-1 were performed for each model configuration.

3.6 Methodological limitations

The experimental program was conducted under active construction and regulatory constraints. Instrumentation was limited, and no pore-pressure measurements were performed. Piling equipment, pile geometry, and regulated pile–piston regime are unique to the investigated project. Accordingly, the findings are valid only for the tested soil profile and operational conditions and should not be generalized without further instrumented studies. The pile load tests followed DSTU (2011), employing stepwise loading with a stabilization criterion of 0.1 mm per 60 min, whereas many EU standards apply cyclic loading or constant-rate-of-penetration. Furthermore, Ukrainian practice relies primarily on static load testing rather than CPT-based site characterization. As a result, parameters such as the small-strain shear modulus and the earth pressure coefficient at rest were not available for direct numerical modelling.

4 RESULTS AND INTERPRETATION

4.1 Pile installation performance

The control piles (P1), installed without jetting, reached refusal at a depth of 6.0 m within the bearing layer EGE-4 (E = 26 MPa) under a maximum pressing force of 1834 kN (187 tf), establishing the baseline soil resistance. The project piles (P2), installed with regulated jetting, reached the target depth of 7.7 m. Additional penetration of 1.7–1.9 m was achieved under the same pressing force. The reduction in installation resistance of 55–69% across the respective soil layers is illustrated in Figure 4.

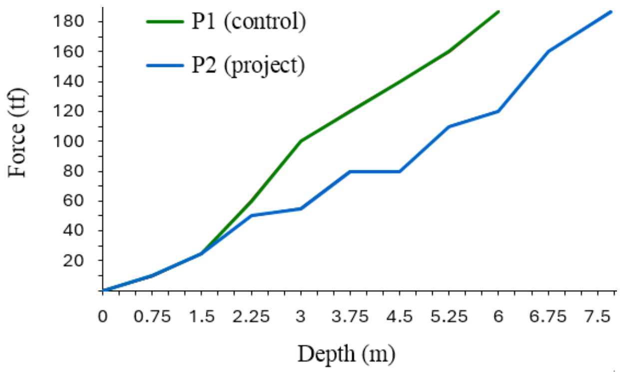

Figure 4. Installation performance of the piles

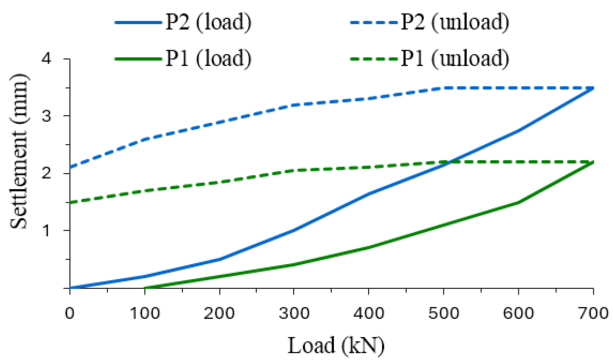

Figure 5. Load-settlement curves for tested piles

Three characteristic drops in soil resistance were observed, corresponding to cyclic stick–slip behavior within sand layers. The spacing of approximately 0.75 m between these drops matches the stroke length of the hydraulic cylinders, indicating mechanical coupling between the jetting cycle and pile advancement. The first onset of this effect occurred at depths of 2.25–3.0 m within layer EGE-2, where the difference between project and control piles reached approximately 45 tf (about 55% of the reference pressing force). A second drop was observed at 3.75–4.5 m (EGE-3), with a relative reduction of about 64%, marking the transition between dense sand sublayers. The most pronounced slip phase occurred at depths of 5.25–6.0 m, where the reduction reached up to 69%. At greater depths, the effect became less pronounced, suggesting a gradual change in soil–hydraulic interaction conditions. These observations are consistent with earlier findings (Shepley and Bolton, 2013), who reported peak pore pressures at depths of 3–4 m, and with (Gillow et al., 2018), who documented similar pressure peaks within the 3–5 m penetration interval in dense sands. Comparable reductions (up to 45%) have also been reported in previous field studies during jet activation within the 3–4 m depth range.

4.2 Assessment of bearing capacity

Static load tests (P3) were conducted in accordance with the officially approved testing program developed by an independent certified organization under applicable standards. Two control (P1) and two jetted (P2) piles were tested. Although the number of formal load tests is limited, continuous installation monitoring was performed for all project piles using the hydraulic system of the pressing machine. The recorded force–depth curves demonstrated consistent resistance mobilization within the dense bearing layer (EGE-4), with no progressive degradation of peak resistance among jetted piles.

Settlements at the maximum applied load of 700 kN were limited to 2.20 mm for the control pile and 3.50 mm for the jetted pile, both well below allowable limits, as illustrated in Figure 5. The allowable axial load determined from testing (466.6 kN) exceeds the design load of 400 kN with a safety factor of 1.2. Within the investigated soil profile and regulated jetting regime, no observable reduction in axial bearing capacity was detected. These results contrast with concerns regarding uncertainty in pile capacity in sands (Malhotra, 2004), where method variability may lead to differences of up to 30–40 % in load-bearing capacity. Given the limited number of static tests, these findings should be interpreted as site-specific confirmation rather than statistical demonstration of equivalence.

4.3 Hypothesized hydraulic mechanism under regulated pile–piston regime

Laboratory-scale studies (Gillow et al., 2018; Liu et al., 2020; Wan et al., 2023) interpret the stick–slip phenomenon as a cyclic process of pore-pressure accumulation and partial dissipation caused by local filtration beneath the pile toe and uncontrolled fluidization, where part of the injected water dissipates into the surrounding soil. In such open hydraulic systems, reported pressure increments do not exceed 0.2–0.4 MPa, generating unloading of approximately 10–20 tf associated with gradual loss of soil-pile contact strength.

Full-scale observations in the present study indicate a different hydrodynamic regime under controlled uplift and pressing cycles. During regulated pile uplift by the pressing machine, a temporarily confined, water-filled cavity forms beneath the pile tip. When pressing resumes, the confined soil–water system provides the boundary conditions necessary for pressure build-up. Once a critical pressure increment is reached, rupture of the sealing slurry layer occurs, generating a short-duration unloading impulse, initiating the slip phase.

Table 1. Summary of installation parameters

Phase	Pile type / quantity (N)	Water jetting regime	Nozzle Ø (mm)	Water use (L/pile)	Max force (kN)	Time (min)	Depth (m)	Stick–slip observed
1	Control (2)	N/A	N/A	N/A	1834	6	6.0	No
2a	Project (8)	Continuous	2.0	200	1834	9–10	7.7	Yes
2b	Project (8)	Pile–piston	2.0	120	1834	21–22	7.7	Yes
4a	M1 (3)	Continuous	2.0	40–45	< 1	5.5	1.2	Yes
4b	M2 (3)	Slurry out	0.7	25	< 1	4	1.2	No

The following formulation represents mechanistic interpretation of the recorded force oscillations. As no pore-pressure transducers were installed beneath the pile toe, cavity pressure values were estimated indirectly by back-calculation from unloading magnitudes. The model therefore constitutes a first-order energetic approximation consistent with observed force drops, rather than a directly measured hydraulic response. The key installation parameters are summarized in Table 1.

4.3.1 Representation of the pile–water–soil system

During the regulated pile–piston cycle, the confined cavity may be idealized as a closed elastic chamber formed beneath the pile tip (pile uplift of 0.3–0.4 m). In this representation, pressure increases with applied pressing force until a critical condition is reached. The critical cavity pressure (1) may be expressed as:

$$P_{crit} = P_0 + \frac{F_{press}}{A_{pile}} \quad (1)$$

where P_0 is the initial cavity pressure (MPa), F_{press} is the pressing force (kN), A_{pile} is the pile base area (m²). For recorded pressing forces of 490–540 kN and a pile base area of 0.1225 m^2, the inferred pressure increment associated with unloading events is on the order of 4 MPa. This estimated pressure rise corresponds to the observed unloading magnitude of approximately 45 tf (441 kN) recorded during the slip phase (Fig. 4). The corresponding impulse force (2) may be expressed as:

$$F_{imp} = \Delta P \cdot A_{pile} \quad (2)$$

where ΔP is the estimated pressure increment between accumulation and rupture. The potential work capacity of the pressurized cavity (3), in first approximation, may be evaluated as:

$$W_{pot} = \Delta P \cdot V_c \quad (3)$$

where V_c is the cavity volume (m^3). For an estimated cavity volume of 0.03 m^3 and a pressure increment of 4 MPa, the stored energy is approximately 120 kJ, consistent in magnitude with the unloading of about 45 tf recorded during the slip phase (Fig. 4).

The proposed piston-type mechanism should be regarded as a hypothesis requiring verification through instrumented field tests with direct pore-pressure measurements. Within this conceptual framework, the transition from stick to slip is interpreted as a hydraulic discharge impulse, in which the pressurized cavity temporarily functions as an energy-storage zone.

Following unloading, pressure rebuilds as the cavity refills, forming a repeatable cycle governed by jetting rate, confinement, and cavity-filling time. During each regulated cycle, the cavity fills at approximately 9 L/min and reaches a pump relief activation pressure of 16 MPa in about 3.5 min, with filtration losses remaining below 5% in EGE-3.

Although the installation time increased to 21 min compared with 10 min in Phase 2a, water consumption decreases by about 40 %, and energy demand is reduced due to the lower flow rate. As summarized in Table 1, lowering the pressing resistance by 55–69% (Phase 2b) reduced the water demand to 120 L/pile. Conventional systems can consume 600–1500 L per metal sheet pile (Gillow et al., 2018) and operate at pump capacities of approximately 20 kW. In contrast, the regulated pile–piston regime achieved stable, localized fluidization at 9 L/min using only 3.1 kW.

4.3.2 Model pile tests

Complementary 1-g model tests (P4) qualitatively reproduced penetration behavior under controlled and continuous jetting conditions without machinery.

Under continuous jetting (Phase 4a), penetration was accompanied by abrupt downward movements indicative of hydraulic instability associated with stick–slip behavior and uncontrolled fluidization. In contrast, regulated jetting with slurry extraction (Phase 4b) produced smoother and more stable penetration.

As summarized in Table 1, water consumption was reduced by approximately 40 % compared with continuous jetting, and oscillatory resistance behavior was substantially mitigated. These observations indicate that penetration stability is governed primarily by flow regulation and effective slurry extraction rather than by absolute pressure or discharge volume.

No force–displacement data or pore-pressure measurements were obtained; therefore, the results are qualitative rather than quantitative. Accordingly, the investigation provides mechanism-oriented support for the hypothesized hydraulic interaction at prototype scale, without aiming to achieve stress-similitude with dense sand conditions.

4.3.3 Stick–slip effect mitigation strategy

Geometric enhancements such as ribs or grooves may compensate for load-bearing capacity losses after water jetting by 30–80 % (Ruver and Bruschi, 2023).

However, such modifications do not address the source of hydraulic instability – the accumulation of excess pore pressure beneath the pile tip, which induces cyclic stick–slip behavior. This instability can be mitigated by employing an anti-plugging geometry (APG) to facilitate controlled slurry extraction beneath the pile toe and prevent hydraulic plugging.

To implement this principle, two design concepts were developed.

For reinforced concrete piles operating under the pile–piston installation regime, cross-slots (2 × 30–50 mm) were introduced at the tip. These slots divide the jet into substreams, reduce hydraulic confinement beneath the toe, protect the nozzle, and promote upward flow along the pile surface. For the ground implant – a newly developed composite structural element (EC Transzvuk, UA patent application No. a202405966, 16.12.2024) – a more integrated APG was implemented, as illustrated in Figure 6.

Figure 6. Ground implant with anti-plugging geometry, where: 1 – cross-slots; 2 – helical grooves; 3 – base.

The system comprises cross-slots (1) at the toe and double-start trapezoidal helical grooves (2) along the base (3). Together with an internal cavity for high-pressure hose insertion, this configuration enables directed nozzle-based water supply and controlled slurry outflow during penetration. The configuration transforms the system from a closed hydraulic regime to a semi-drained state, preventing local oversaturation and ensuring stable penetration.

Both concepts aim to regulate hydraulic conditions beneath the pile tip, limit pore-pressure build-up, and enable controlled, reversible fluidization.

5 FUTURE RESEARCH AND APPLICABILITY

Future research should address the methodological limitations of the present study through instrumented field testing with direct pore-pressure measurements beneath the pile toe. Development of a fluid–structure interaction (FSI) model (Wen et al., 2023) would allow quantification of transient hydraulic processes and verification of the proposed piston-type interpretation.

Complementary numerical modelling approaches (Grabe and Heins, 2017) may assist in evaluating jetting parameters, penetration stability, and soil response under controlled hydraulic regimes.

Additional full-scale tests are required to verify the efficiency of the anti-plugging geometry (APG) to confirm its applicability under different soil conditions. The regulated pile–piston regime and associated piling equipment configuration remain specific to the documented project and require independent validation prior to broader application.

The experimentally observed reduction in pressing resistance suggests the potential for downsizing the developed SO-450 pile-pressing machine. Preliminary engineering assessment indicates that a configuration with a total mass on the order of ≤70 tf and inclination capability up to 15° may be feasible. The proposed concept integrates with an aggregate-modular skid system enabling transverse movement of the pile-pressing machine within a space-grid framework (Meshcheriakov and Andryushchenko, 2023). Such integration, previously constrained by equipment mass, aligns with international coordination principles (ISO, 1984) and current digitalization trends in foundation engineering (Nozaki and Kusakabe, 2022), particularly for modular low- to mid-rise structures.

Future research will focus on the development of an intelligent control module for dynamic regulation of water supply and slurry management, subject to further experimental validation. The regulated water-jet-assisted pile-pressing method and the ground implant incorporating APG may be considered for vibration-sensitive environments, provided that site-specific geotechnical verification is performed.

6 CONCLUSIONS

This study documents prototype-scale hydraulic interaction during regulated water-jet-assisted pile pressing in dense sand under actual construction conditions. The field program demonstrated that regulated jetting reduces pressing resistance by 55–70 % and enables additional penetration of up to 1.7 m under a maximum pressing force of 1834 kN.

A piston-type hydraulic hypothesis is proposed to interpret the observed stick–slip oscillations during pile penetration. Although cavity pressure beneath the pile toe was not directly measured, back-calculated pressure increments are consistent with the recorded force drops and provide a first-order energetic interpretation of the mechanism.

Static load tests conducted in accordance with the approved testing program indicate that no observable reduction in axial bearing capacity occurred under the applied jetting regime for the investigated soil profile. Settlements under 700 kN remained below 3.5 mm, and the allowable load of 466.6 kN exceeded the design value of 400 kN with a safety factor of 1.2, contrasting with reported concerns regarding potential capacity loss associated with water jetting. Continuous installation monitoring based on machine-recorded force–depth data provided quasi-statistical evidence of repeatable soil resistance throughout penetration.

Complementary mechanism-oriented 1-g tests qualitatively demonstrated that regulated jetting with slurry removal mitigates the stick–slip effect and reduces water consumption by approximately 40 % compared with continuous jetting. These tests were not intended to reproduce stress conditions in dense sand but to examine hydraulic instability mechanisms and operability of the anti-plugging geometry.

Within the investigated framework, the results constitute field-validated evidence of a controllable hydraulic interaction mechanism under construction constraints and establish a technically substantiated basis for future instrumented field and laboratory investigations including direct pore-pressure measurements, as well as for stress-scaled physical modelling aimed at quantitative verification of the underlying installation mechanism.

REFERENCES

Gillow, M., Haigh, S., Ishihara, Y., Ogawa, N., & Okada, K. (2018). Water Jetting for Sheet Piling. In Proceedings of the First International Conference on Press-in Engineering, Kochi, Japan, pp. 335-342.

Grabe, J. & Heins, E. (2017). Coupled deformation–seepage analysis of dynamic capacity tests on open-ended piles in saturated sand. Acta Geotechnica, 12(1), 211–223. https://doi.org/10.1007/s11440-016-0442-z

ISO 2848:1984 (1984). Building construction — Modular coordination — Principles and rules. International Organization for Standardization.

Gunaratne, M., Hameed, R. A., Kuo, C., Reddy, D. V., & Putcha, S. (1999). Investigation of the effects of pile jetting and preforming. Report No. FL/DOT/RMC/B-9479, Report 772. FL-DOT & FHWA. https://rosap.ntl.bts.gov/view/dot/15679

Liu, X., Zhang, Y., Chen, B., & Wang, J. (2020). Stick–slip behavior during jacked pile tests in soft clays. Acta Geotechnica, 15(2), 559–572. https://doi.org/10.1007/s11440-019-00841-2

Maiti, R., & Shepley, P. (2025). Penetration of jet piles on submerged granular beds. Ocean Eng., 315, 119914. https://doi.org/10.1016/j.oceaneng.2024.119914

Malhotra, S. (2004). Axial capacity of pipe piles in sand. In Proceedings of the Geo-Trans 2004, Geotechnical Engineering for Transportation Projects, Special Publication No. 126, Saint Petersburg, pp. 27-31.

Meshcheriakov, G.N., & Andryushchenko, A.M. (2023). Automated construction process for foundation engineering. In Proceedings of the 40th ISARC, India, Waterloo: IAARC Publications, pp. 172-179. https://doi.org/10.22260/ISARC2023/0025

Mezzomo, F. (2009). Experimental study of piles driven with the assistance of a water jet. Master's Dissertation, Federal University of Rio Grande do Sul, Brazil. https://lume.ufrgs.br/handle/10183/18809

Nozaki, T., & Kusakabe, O. (2022). The Future Vision of Press-in Technology. IPA Newsletter, 7(1), 43-57.

Passini, L. de B., & Schnaid, F. (2015). Experimental investigation of pile installation by vertical jet fluidization in sand. Journal of Offshore Mechanics and Arctic Engineering, 137(4), 041901. https://doi.org/10.1115/1.4030707

Passini, L., Rocha, M., Möller, S., Schnaid, F. (2018). Mechanism of model pile installation by water-jet fluidization in sand. Ocean Engineering, 170(1): 160–170. https://doi.org/10.1016/j.oceaneng.2018.10.017

Ruver, C. A., & Bruschi, G. J. (2023). Mechanical and numerical behavior of water jet-driven under-reamed concrete piles. Soils and Rocks, 46(2), e2023012822. https://doi.org/10.28927/SR.2023.012822

Shepley, P., & Bolton, M. D. (2013). Centrifuge modeling of driven piles in sand: Influence of saturation. Int. Journal of Physical Modelling in Geotechnics, 13(1), 24–35. https://doi.org/10.1680/ijpmg.12.00014

Tsinker, G. P. (1988). Pile jetting. Journal of Geotechnical Engineering, 114(3), 326–334.

DSTU B V.2.1-27:2010 (2011). Piles. Determination of bearing capacity based on field test results. Kyiv: Ministry of Regional Development, Construction, Housing and Communal Services of Ukraine.

US Army Corps of Engineers (USACE). (1962). Use of jetting during pile driving. Technical Memorandum 3-406, Waterways Experiment Station, Mississippi.

Wen, K., Kontoe, S., & Jardine, R. J. (2023). An axial load transfer model for piles driven in chalk. Journal of Geotechnical and Geoenvironmental Engineering (ASCE), 149(11), 04023120. https://doi.org/10.1061/(ASCE)GT.1943-5606.0003131

White, D.J., & Bolton, M.D. (2004). Centrifuge modelling of pile installation. Géotechnique, 54(6), 375–386. https://doi.org/10.1680/geot.2004.54.6.375